Resonance $X(3960)$ as a hidden charm-strange scalar tetraquark

S. S. Agaev,[1] K. Azizi,[2,3,*] and H. Sundu[4,5]

[1]*Institute for Physical Problems, Baku State University, Az-1148 Baku, Azerbaijan*
[2]*Department of Physics, University of Tehran, North Karegar Avenue, Tehran 14395-547, Iran*
[3]*Department of Physics, Doğuş University, Dudullu-Ümraniye, 34775 Istanbul, Turkey*
[4]*Department of Physics, Kocaeli University, 41380 Izmit, Turkey*
[5]*Department of Physics Engineering, Istanbul Medeniyet University, 34700 Istanbul, Turkey*

(Received 20 December 2022; accepted 16 February 2023; published 13 March 2023)

We investigate features of the hidden charm-strange scalar tetraquark $c\bar{c}s\bar{s}$ by calculating its spectral parameters and width, and we compare the obtained results with the mass and width of the resonance $X(3960)$ discovered recently in the LHCb experiment. We model the tetraquark as a diquark-antidiquark state $X=[cs][\bar{c}\bar{s}]$ with spin-parities $J^{\mathrm{PC}}=0^{++}$. The mass and current coupling of X are calculated using the QCD two-point sum rules by taking into account various vacuum condensates up to dimension 10. The width of the tetraquark X is estimated via the decay channels $X\to D_s^+D_s^-$ and $X\to\eta_c\eta^{(\prime)}$. The partial widths of these processes are expressed in terms of couplings G, g_1, and g_2, which describe the strong interactions of particles at the vertices $XD_s^+D_s^-$, $X\eta_c\eta'$, and $X\eta_c\eta$, respectively. Numerical values of G, g_1, and g_2 are evaluated by employing the three-point sum rule method. Comparing the results $m=(3976\pm 85)$ MeV and $\Gamma_{\mathrm{X}}=(42.2\pm 12.0)$ MeV obtained for parameters of the tetraquark X and experimental data of the LHCb Collaboration, we conclude that the resonance $X(3960)$ can be considered as a candidate to a scalar diquark-antidiquark state.

DOI: 10.1103/PhysRevD.107.054017

I. INTRODUCTION

Recently, the LHCb Collaboration reported the observation of a new threshold peaking structure $X(3960)$ in the $D_s^+D_s^-$ invariant mass distribution in the $B^+\to D_s^+D_s^-K^+$ decay [1]. Performed analysis demonstrated that it is a scalar resonance $J^{\mathrm{PC}}=0^{++}$ with mass and width

$$m_{\mathrm{exp}}=3956\pm 5\pm 10\ \mathrm{MeV},$$
$$\Gamma_{\mathrm{exp}}=43\pm 13\pm 8\ \mathrm{MeV}. \qquad (1)$$

The collaboration also found an additional structure around 4140 MeV with spin-parities 0^{++}. The resonance $X(3960)$ was interpreted by LHCb as a four-quark state with the content $c\bar{c}s\bar{s}$, whereas the structure 4140 MeV may be either a new resonance or a $J/\psi\phi\leftrightarrow D_s^+D_s^-$ coupled-channel effect.

Four-quark exotic mesons composed of quarks $c\bar{c}s\bar{s}$ with different quantum numbers are not something new for either experimental or theoretical physicists. In fact, resonances with the quark content $c\bar{c}s\bar{s}$ were fixed by LHCb in the $J/\psi\phi$ invariant mass distribution in the process $B^+\to J/\psi\phi K^+$ [2]. The discovered states $X(4140)$ and $X(4274)$ are axial-vector particles with $J^{\mathrm{PC}}=1^{++}$, whereas the spin-parities of $X(4500)$ and $X(4700)$ are $J^{\mathrm{PC}}=0^{++}$. It should be noted that the resonances $X(4140)$ and $X(4274)$ were previously seen by the CDF Collaboration [3] in the decays $B^\pm\to J/\psi\phi K^\pm$ and confirmed later by CMS [4] and D0 experiments [5]. The scalar structures $X(4500)$ and $X(4700)$ were fixed by the LHCb Collaboration for the first time.

In experiments, numerous exotic vector mesons built of $c\bar{c}s\bar{s}$ quarks were observed as well. Thus, the state $Y(4660)$ was found for the first time by the Belle Collaboration in the process $e^+e^-\to\gamma_{\mathrm{ISR}}\psi(2S)\pi^+\pi^-$ as one of two resonant structures in the $\psi(2S)\pi^+\pi^-$ invariant mass distribution. Because $Y(4660)$ was produced in the e^+e^- annihilation, its quantum numbers are $J^{\mathrm{PC}}=1^{--}$. The structure $X(4630)$ was discovered by LHCb in the $J/\psi\phi$ invariant mass distribution of the decay $B^+\to J/\psi\phi K^+$ [6].

Theoretical studies of four-quark states $c\bar{c}s\bar{s}$ also have a rich history. The charmoniumlike exotic mesons with a $s\bar{s}$ component were investigated by means of different methods in numerous publications (see, as examples, Refs. [7–11]). Comprehensive analyses of some hidden-charm diquark-antidiquark systems $[cs][\bar{c}\bar{s}]$ were carried out in our articles as well. Thus, the axial-vector resonances $X(4140)$ and

*Corresponding author.
kazem.azizi@ut.ac.ir

$X(4274)$ were investigated in Ref. [12], in which we treated them as diquark-antidiquark states built of scalar and axial-vector components belonging to triplet and sextet representations of the $SU_c(3)$ color group, respectively. We not only calculated their masses and current couplings (or pole residues), but also evaluated full widths of these tetraquarks. Predictions for parameters of the color-triplet diquark-antidiquark state allowed us to interpret it as the resonance $X(4140)$. Contrary to this, the full width of the tetraquark with color sextet ingredients is considerably wider than that of the resonance $X(4274)$. Therefore, to explain the internal organization of $X(4274)$, alternative models should be examined, though existence of a new axial-vector resonance with the mass $m \approx 4274$ MeV and full width $\Gamma \approx 200$ MeV cannot be excluded.

The vector resonance $Y(4660)$ was studied as a diquark-antidiquark vector state $[cs][\bar{c}\bar{s}]$ with $J^{\mathrm{PC}} = 1^{--}$ in our work [13]. Results obtained there for the mass and full width of this structure made it possible to interpret the resonance $Y(4660)$ as the diquark-antidiquark exotic meson. The detailed analysis of $X(4630)$ was performed in Ref. [14] by assuming that it is a vector tetraquark $[cs][\bar{c}\bar{s}]$ with spin-parities $J^{\mathrm{PC}} = 1^{-+}$. Here, a nice agreement was obtained between the LHCb data for parameters of the resonance $X(4630)$ and theoretical predictions of the diquark-antidiquark model. There are numerous articles devoted to experimental studies and theoretical analysis of hidden charm-strange four-quark mesons in the literature: A relatively full list of such publications can be found in Refs. [1,12–14].

The first announcement made in Ref. [15] about the discovery of the resonance $X(3960)$ triggered extreme interest in this state. In papers that appeared afterwards [16–22], authors addressed different aspects of its internal organization, production mechanisms, and rates, placing $X(3960)$ into various four-quark multiplets. The coupled-channel explanation of $X(3960)$ was suggested in Ref. [16], where it emerges as an enhancement in the $D_s^+ D_s^-$ mass distribution via interaction of the $D^+ D^-$ and $D_s^+ D_s^-$ coupled channels. In Ref. [18], the authors assigned $X(3960)$ the hadronic molecule $D_s^+ D_s^-$ and performed studies in the context of the sum rule method. The resonance $X(3960)$ was explained also as near the $D_s^+ D_s^-$ threshold enhancement due to the contribution of the conventional P-wave charmonium $\chi_{c0}(2P)$ [21].

In the present article, we explore the tetraquark $X = [cs][\bar{c}\bar{s}]$ with spin-parities $J^{\mathrm{PC}} = 0^{++}$ and compute its parameters. The mass and current coupling of X are evaluated using the QCD two-point sum rule method. Its full width is estimated using the decay channels $X \to D_s^+ D_s^-$ and $X \to \eta_c \eta^{(\prime)}$. Partial widths of these processes are expressed through strong couplings G, g_1, and g_2 of particles at the vertices $X D_s^+ D_s^-$, $X\eta_c\eta'$, and $X\eta_c\eta$, respectively. To calculate G, g_1, and g_2, we employ technical tools of the three-point sum rule approach. Results found for parameters of the state X are confronted with the LHCb data to verify the diquark-antidiquark model for $X(3960)$.

This paper is organized in the following way: In Sec. II, we compute the mass and current coupling of the tetraquark X by means of the QCD two-point sum rule method. The decay $X \to D_s^+ D_s^-$ is studied in Sec. III, where we calculate the coupling G and partial width of this process. The strong couplings g_1 and g_2 and partial widths of the decays $X \to \eta_c\eta'$ and $X \to \eta_c\eta$, as well as the full width of X, are found in Sec. IV. Section V is reserved for our concluding notes.

II. MASS AND CURRENT COUPLING OF THE TETRAQUARK X

In this section, we consider the scalar diquark-antidiquark state $X = [cs][\bar{c}\bar{s}]$ and extract its spectroscopic parameters from the two-point sum rule analysis [23,24]. It is known that the sum rule method operates with correlation functions and interpolating currents of the particles under investigation. There are different ways to construct a scalar tetraquark and corresponding current using a diquark and an antidiquark with different spin-parities [25]. Thus, one may construct such a state using the pseudoscalar $c^T C s$ or vector $c^T C\gamma_\mu\gamma_5 s$ diquarks and corresponding antidiquarks, where C is the charge-conjugation operator. However, we assume that X is built of a scalar diquark $c^T C\gamma_5 s$ and antidiquark $\bar{c}\gamma_5 C\bar{s}^T$: The reason is that the scalar diquark (antidiquark) configuration is the most attractive and stable two-quark system [26].

The structures $\epsilon c^T C\gamma_5 s$ and $\tilde{\epsilon}\bar{c}\gamma_5 C\bar{s}^T$ are the color antitriplet and triplet states of the color $SU_c(3)$ group, respectively. Then the interpolating current for the tetraquark X has the form

$$J(x) = \epsilon\tilde{\epsilon}[c_b^T(x) C\gamma_5 s_c(x)][\bar{c}_m(x)\gamma_5 C\bar{s}_n^T(x)], \qquad (2)$$

where $\epsilon\tilde{\epsilon} = \epsilon^{abc}\epsilon^{amn}$ and a, b, c, m, and n are color indices. This current belongs to the $[\bar{\mathbf{3}}_c]_{cs} \otimes [\mathbf{3}_c]_{\bar{c}\bar{s}}$ representation of the color group and corresponds to the scalar state with quantum numbers $J^{\mathrm{PC}} = 0^{++}$. The current $J(x)$ describes the ground-state scalar particle with lowest mass and required spin-parities.

The mass m and coupling f of the tetraquark X can be determined from analysis of the correlation function $\Pi(p)$,

$$\Pi(p) = i\int d^4x e^{ipx}\langle 0|\mathcal{T}\{J(x)J^\dagger(0)\}|0\rangle. \qquad (3)$$

To derive the required sum rules, one has to express $\Pi(p)$ using the spectroscopic parameters of the tetraquark X. For these purposes, we insert into the correlation function $\Pi(p)$ a complete set of states with quantum numbers 0^{++} and perform integration over x in Eq. (3). As a result, we get

$$\Pi^{\mathrm{Phys}}(p) = \frac{\langle 0|J|X(p)\rangle\langle X(p)|J^\dagger|0\rangle}{m^2 - p^2} + \cdots. \qquad (4)$$

The obtained expression forms a hadronic representation of $\Pi(p)$ and is the phenomenological (physical) side of the sum rule. Here, the contribution coming from the ground-state particle X is written down explicitly, whereas contributions of higher resonances and continuum states are denoted by the ellipses.

The function $\Pi^{\rm Phys}(p)$ can be further simplified by employing the matrix element

$$\langle 0|J|X(p)\rangle = fm. \tag{5}$$

It is easy to find that, in terms of the parameters m and f, the function $\Pi^{\rm Phys}(p)$ takes the following form:

$$\Pi^{\rm Phys}(p) = \frac{m^2 f^2}{m^2 - p^2} + \cdots. \tag{6}$$

The $\Pi^{\rm Phys}(p)$ function has a simple Lorentz structure proportional to I, and the relevant invariant amplitude $\Pi^{\rm Phys}(p^2)$ is given by the rhs of Eq. (6).

To determine the QCD side of the sum rules $\Pi^{\rm OPE}(p)$, we use the interpolating current $J(x)$ in Eq. (3) and contract the heavy and light quark fields. After simple manipulations, we obtain

$$\Pi^{\rm OPE}(p) = i\int d^4x e^{ipx}\epsilon\tilde{\epsilon}\epsilon'\tilde{\epsilon}'{\rm Tr}\left[\gamma_5\tilde{S}_c^{bb'}(x)\right.$$
$$\left.\times\gamma_5 S_s^{cc'}(x)\right]{\rm Tr}\left[\gamma_5\tilde{S}_s^{n'n}(-x)\gamma_5 S_c^{m'm}(-x)\right], \tag{7}$$

where $S_c(x)$ and $S_s(x)$ are the c- and s-quark propagators, respectively. Explicit expressions of these propagators are presented in the Appendix (see also Ref. [27]). In Eq. (7), we have also used the notation

$$\tilde{S}_{c(s)}(x) = CS^T_{c(s)}(x)C. \tag{8}$$

The correlation function $\Pi^{\rm OPE}(p)$ should be computed in the operator product expansion (OPE) with some accuracy. $\Pi^{\rm OPE}(p)$ also has a trivial structure ~I and is characterized by an amplitude $\Pi^{\rm OPE}(p^2)$. Having equated the invariant amplitudes $\Pi^{\rm Phys}(p^2)$ and $\Pi^{\rm OPE}(p^2)$, one gets the master QCD sum rule equality. Afterwards, one needs to suppress contributions of higher resonances and continuum states by applying the Borel transformation. The assumption about quark-hadron duality allows one to subtract these suppressed terms from the obtained expression. After these operations, the sum rule equality starts to depend on the Borel M^2 and continuum threshold s_0 parameters.

The Borel transformation of $\Pi^{\rm Phys}(p^2)$ is a simple function, whereas for $\Pi^{\rm OPE}(p^2)$ we get a complicated formula

$$\Pi(M^2, s_0) = \int_{4\mathcal{M}^2}^{s_0} ds\rho^{\rm OPE}(s)e^{-s/M^2} + \Pi(M^2), \tag{9}$$

where $\mathcal{M} = m_c + m_s$. In numerical computations, we set $m_s^2 = 0$, but we include in our analysis terms proportional to m_s. The two-point spectral density $\rho^{\rm OPE}(s)$ is calculated as an imaginary part of the correlation function. The second term, $\Pi(M^2)$, includes nonperturbative contributions extracted directly from $\Pi^{\rm OPE}(p)$. The correlator $\Pi(M^2, s_0)$ is computed by taking into account nonperturbative terms up to dimension 10. Explicit expression of $\Pi(M^2, s_0)$ is written down in the Appendix.

The sum rules for m and f are expressed via the invariant amplitude $\Pi(M^2, s_0)$,

$$m^2 = \frac{\Pi'(M^2, s_0)}{\Pi(M^2, s_0)}, \tag{10}$$

and

$$f^2 = \frac{e^{m^2/M^2}}{m^2}\Pi(M^2, s_0), \tag{11}$$

where $\Pi'(M^2, s_0) = d\Pi(M^2, s_0)/d(-1/M^2)$.

To carry out the numerical computations in accordance with Eqs. (10) and (11), we have to fix values of different vacuum condensates. The reason is that the sum rules for m^2 and f^2 through $\Pi(M^2, s_0)$ depend on the vacuum expectation values of quark, gluon, and mixed operators. The vacuum condensates that enter into the sum rules [Eqs. (10) and (11)] are universal quantities obtained from analysis of various hadronic processes [23,24,28–30]:

$$\begin{aligned}
&\langle\bar{q}q\rangle = -(0.24\pm0.01)^3\,{\rm GeV}^3, \quad \langle\bar{s}s\rangle = (0.8\pm0.1)\langle\bar{q}q\rangle,\\
&\langle\bar{s}g_s\sigma Gs\rangle = m_0^2\langle\bar{s}s\rangle, \quad m_0^2 = (0.8\pm0.1)\,{\rm GeV}^2,\\
&\langle\frac{\alpha_s G^2}{\pi}\rangle = (0.012\pm0.004)\,{\rm GeV}^4,\\
&\langle g_s^3 G^3\rangle = (0.57\pm0.29)\,{\rm GeV}^6,\\
&m_c = (1.27\pm0.02)\,{\rm GeV}, \quad m_s = 93^{+11}_{-5}\,{\rm MeV}.
\end{aligned} \tag{12}$$

It is seen that the vacuum condensate of the strange quark differs from $\langle 0|\bar{q}q|0\rangle$ [28]. The mixed condensates $\langle\bar{q}g_s\sigma Gq\rangle$ and $\langle\bar{s}g_s\sigma Gs\rangle$ are expressed in terms of the corresponding quark condensates and the parameter m_0^2. The numerical value of the latter was extracted from the analysis of baryonic resonances in Ref. [29]. For the gluon condensate $\langle g^3G^3\rangle$, we use the estimate given in Ref. [30]. This list also contains the masses of c and s quarks in the $\overline{\rm MS}$ scheme from Ref. [31].

Predictions for m and f extracted from the sum rules depend also on the Borel and continuum subtraction parameters M^2 and s_0. In general, physical quantities should not contain residual effects connected with the choice of M^2. But in a real situation, m and f bear imprints of operations fulfilled to isolate contribution of the ground-state particle to sum rules. A way to solve this problem is by using some prescriptions to minimize the unwanted effects. To this end, in the sum rule analysis, the choice of a working window for the Borel parameter M^2 is restricted by the dominance of the pole contribution (PC) and convergence of OPE. To quantify these constraints, it is convenient to introduce the expressions

$$\mathrm{PC} = \frac{\Pi(M^2, s_0)}{\Pi(M^2, \infty)} \tag{13}$$

and

$$R(M^2) = \frac{\Pi^{\mathrm{DimN}}(M^2, s_0)}{\Pi(M^2, s_0)}. \tag{14}$$

The first of them is a measure of the pole contribution and is necessary to find the higher border of the M^2 region. In Eq. (14), $\Pi^{\mathrm{DimN}}(M^2, s_0)$ indicates the last three terms in the OPE of $\Pi(M^2, s_0)$: i.e., $\mathrm{DimN} = \mathrm{Dim}(8+9+10)$. We use $R(M^2)$ to estimate the convergence of OPE and fix a lower limit of M^2.

In working regions of M^2 and s_0, the perturbative contribution to the correlation function $\Pi(M^2, s_0)$ has to be larger than those due to nonperturbative terms. Besides, the window for M^2 should generate stable predictions for the extracted physical quantities. The performed analysis demonstrates that the windows for M^2 and s_0, which satisfy these constraints, are

$$M^2 \in [3, 4]\ \mathrm{GeV}^2, \qquad s_0 \in [21, 22]\ \mathrm{GeV}^2. \tag{15}$$

Indeed, in the regions given by Eq. (15), the pole contribution varies on average within the interval

$$0.80 \geq \mathrm{PC} \geq 0.49. \tag{16}$$

In Fig. 1, the PC is drawn as a function of the Borel parameter at various values of s_0. It is seen that except for a small domain $M^2 > 2.8\ \mathrm{GeV}^2$ at $s_0 = 21\ \mathrm{GeV}^2$, the dominance of the pole contribution—i.e., the constraint $\mathrm{PC} \geq 0.5$—is fulfilled for all values of the parameters M^2 and s_0.

In Fig. 2, we demonstrate the dependence on M^2 of the perturbative and different nonperturbative contributions to $\Pi(M^2, s_0)$. It is evident that the perturbative term is considerably larger than the nonperturbative contributions, and it constitutes 80% of $\Pi(M^2, s_0)$ at $M^2 = 3\ \mathrm{GeV}^2$. This figure confirms also the convergence of the OPE, which implies that the contributions of the nonperturbative terms reduce by increasing the dimensions of the corresponding operators. The Dim3 term numerically exceeds the contributions of other nonperturbative operators, whereas the Dim9 and Dim10 terms are very small and not shown in the plot. The quantity $R(M^2)$ at $M^2 = 3\ \mathrm{GeV}^2$ is less than 0.01, which proves numerically the convergence of the OPE and correctness of the lower value of M^2.

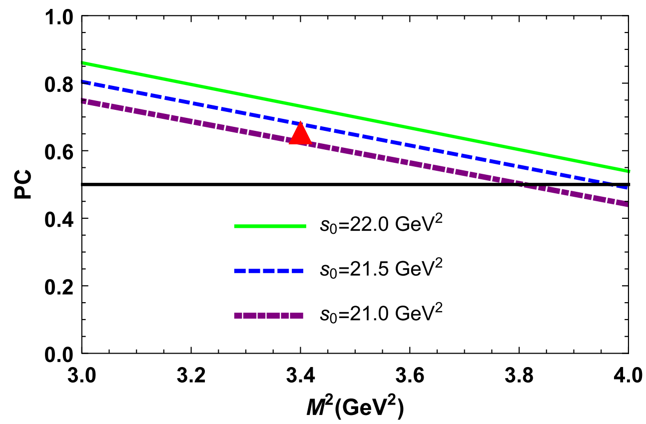

FIG. 1. Pole contribution as a function of the Borel parameter M^2 at various s_0 values. The horizontal black line limits a region $\mathrm{PC} = 0.5$. The red triangle fixes the point where the mass m of the tetraquark X has effectively been extracted.

The residual dependences of the mass m of the tetraquark X on the Borel and continuum subtraction parameters M^2 and s_0 are shown in Fig. 3. It is seen that the window for M^2, where parameters of X are extracted, leads to approximately stable predictions for m. At the same time, one observes some variations of m against the Borel parameter M^2. This effect allows us to estimate the uncertainties of the sum rule predictions. Variation of the continuum threshold parameter s_0 is another source of the theoretical ambiguities. The region for s_0 has to meet the constraints coming from the dominance of PC and convergence of the OPE. The parameter $\sqrt{s_0}$ also bears information on the mass m^*

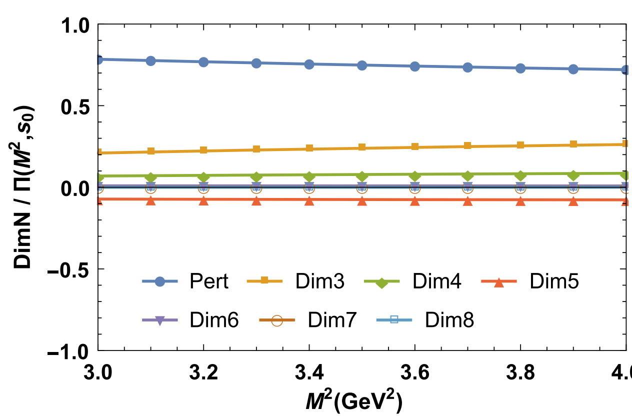

FIG. 2. Different contributions to $\Pi(M^2, s_0)$ normalized to 1 as functions of the Borel parameter M^2. All lines in this figure have been calculated at $s_0 = 21.5\ \mathrm{GeV}^2$.

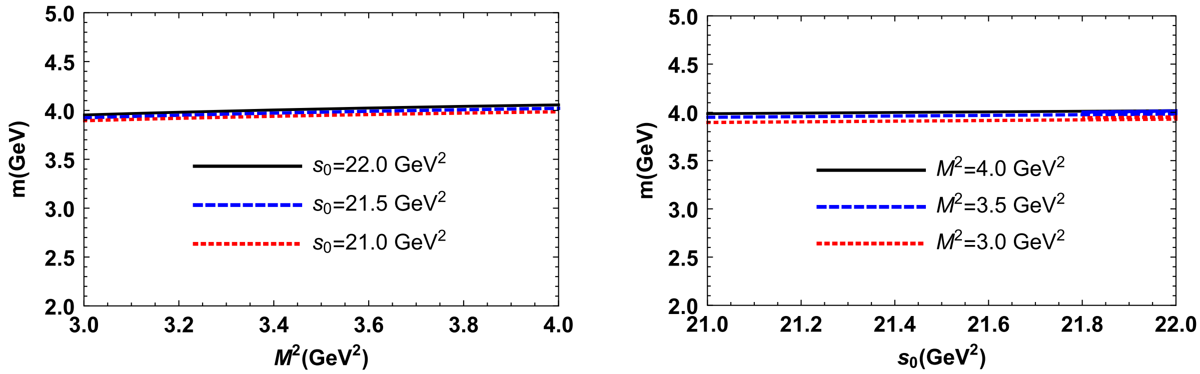

FIG. 3. Mass m of the tetraquark X as a function of the Borel M^2 (left), and as a function of the continuum threshold s_0 parameters (right).

of the first radial excitation of the tetraquark X, and it should obey $\sqrt{s_0} \leq m^*$.

The results for the mass m and coupling f are evaluated as the mean values of these quantities calculated in the working regions [Eq. (15)]:

$$m = (3976 \pm 85)\ \text{MeV},$$
$$f = (7.3 \pm 0.8) \times 10^{-3}\ \text{GeV}^4. \tag{17}$$

The mass and coupling written down in Eq. (17) effectively correspond to the sum rule predictions at $M^2 = 3.4\ \text{GeV}^2$ and $s_0 = 21.5\ \text{GeV}^2$, shown in Fig. 1 by the red triangle. This point is located approximately at the middle of the working regions, where the pole contribution is $\text{PC} \approx 0.64$. This fact, and other details discussed above, guarantees the ground-state nature of X and credibility of the final results. An estimate for the mass of the excited tetraquark $m^* \geq (m + 650)$ MeV stemming from Eqs. (15) and (17) is also reasonable for the double-heavy tetraquarks.

III. DECAY $X \to D_s^+ D_s^-$

The spectroscopic parameters of the tetraquark X form a basis to determine its kinematically allowed decay channels. Because $X(3960)$ was observed in the $D_s^+ D_s^-$ invariant mass distribution, we treat the decay $X \to D_s^+ D_s^-$ as a dominant mode of X. The two-meson threshold for this process $\approx$3937 MeV is below the mass of X. Other decay channels that should be considered in this paper are $X \to \eta_c \eta'$ and $X \to \eta_c \eta$. The kinematical limits for realization of these processes do not exceed $\approx$3941 MeV, which is less than m as well. It is easy to see also that decays of the scalar tetraquark with spin-parities $J^{\text{PC}} = 0^{++}$ to two pseudoscalar mesons with $J^{\text{PC}} = 0^{-+}$ preserves the spin and quantum numbers P and C of the initial state X.

The partial width of the decay $X \to D_s^+ D_s^-$ is determined by a coupling G that describes the strong interaction at the vertex $XD_s^+ D_s^-$. Apart from G, it depends also on the masses and decay constants of the initial and final particles. The mass and coupling of X have been calculated in the present article, whereas physical parameters of the mesons D_s^+ and D_s^- are known from other sources. Therefore, the only physical quantity to be found here is the strong coupling G.

To evaluate G, we use the QCD three-point sum rule method and start our analysis from the correlation function

$$\Pi(p, p') = i^2 \int d^4x d^4y e^{i(p'y - px)} \langle 0 | \mathcal{T}\{ J^{D_s^+}(y) \times J^{D_s^-}(0) J^\dagger(x) \} | 0 \rangle, \tag{18}$$

where $J(x)$, $J^{D_s^+}(y)$, and $J^{D_s^-}(0)$ are the interpolating currents for the tetraquark X and the pseudoscalar mesons D_s^+ and D_s^-, respectively. The four-momenta of X and D_s^+ are denoted by p and p', whereas the momentum of the meson D_s^- is equal to $q = p - p'$. The current $J(x)$ is given by Eq. (2), whereas for the mesons, we use the following currents:

$$J^{D_s^+}(x) = \bar{s}_j(x) i\gamma_5 c_j(x),$$
$$J^{D_s^-}(x) = \bar{c}_i(x) i\gamma_5 s_i(x), \tag{19}$$

with i and j being the color indices.

To continue our study of the strong coupling G, we follow usual recipes of the sum rule method and compute the correlation function $\Pi(p, p')$. To this end, we employ the physical parameters of the tetraquark and mesons participating in this process. The correlator $\Pi(p, p')$ found this way constitutes the phenomenological side $\Pi^{\text{Phys}}(p, p')$ of the sum rule. It is not difficult to see that

$$\Pi^{\text{Phys}}(p, p') = \frac{\langle 0 | J^{D_s^+} | D_s^+(p') \rangle \langle 0 | J^{D_s^-} | D_s^-(q) \rangle}{(p^2 - m^2)(p'^2 - m_{D_s}^2)} \times \frac{\langle D_s^-(q) D_s^+(p') | X(p) \rangle \langle X(p) | J^\dagger | 0 \rangle}{(q^2 - m_{D_s}^2)} + \cdots, \tag{20}$$

where m_{D_s} is the mass of the mesons $D_s^{\pm}$. To derive Eq. (20), we isolate the contribution of the ground-state particles from those due to higher resonances and continuum states. In Eq. (20), the ground-state term is presented explicitly, whereas the dots stand for the other contributions.

The function $\Pi^{\rm Phys}(p,p')$ can be modified by employing the matrix elements of the mesons $D_s^{\pm}$

$$\langle 0|J^{D_s^{\pm}}|D_s^{\pm}\rangle = \frac{m_{D_s}^2 f_{D_s}}{m_c+m_s}, \tag{21}$$

with f_{D_s} being their decay constants. The vertex $XD_s^+D_s^-$ is modeled as

$$\langle D_s^-(q)D_s^+(p')|X(p)\rangle = G(q^2)p\cdot p'. \tag{22}$$

Using these matrix elements, one can easily find a new expression for $\Pi^{\rm Phys}(p,p')$:

$$\Pi^{\rm Phys}(p,p') = G(q^2)\frac{m_{D_s}^4 f_{D_s}^2 fm}{(m_c+m_s)^2(p^2-m^2)} \times \frac{1}{(p'^2-m_{D_s}^2)(q^2-m_{D_s}^2)} \times \frac{m^2+m_{D_s}^2-q^2}{2}+\cdots. \tag{23}$$

The double Borel transformation of the correlation function $\Pi^{\rm Phys}(p,p')$ over variables p^2 and p'^2 is given by the formula

$$\mathcal{B}\Pi^{\rm Phys}(p,p') = G(q^2)\frac{m_{D_s}^4 f_{D_s}^2 fm}{(m_c+m_s)^2(q^2-m_{D_s}^2)}e^{-m^2/M_1^2} \times e^{-m_{D_s}^2/M_2^2}\frac{m^2+m_{D_s}^2-q^2}{2}+\cdots. \tag{24}$$

The correlator $\Pi^{\rm Phys}(p,p')$ and its Borel transformation have a simple Lorentz structure which is proportional to I. As a result, the relevant invariant amplitude $\Pi^{\rm Phys}(p^2,p'^2,q^2)$ is determined by the whole expression written down in Eq. (23).

To derive the QCD side of the three-point sum rule, we express $\Pi(p,p')$ in terms of the quark propagators, and get

$$\Pi^{\rm OPE}(p,p') = \int d^4x d^4y e^{i(p'y-px)}\epsilon\tilde{\epsilon} \times {\rm Tr}\left[\gamma_5\tilde{S}_c^{ib}(y-x)\gamma_5\tilde{S}_s^{ni}(x-y)\gamma_5 S_c^{mj}(x) \times\gamma_5 S_s^{jc}(-x)\right]. \tag{25}$$

The correlator $\Pi^{\rm OPE}(p,p')$ is computed by taking into account the nonperturbative contributions up to dimension 6. This function contains the same trivial Lorentz structure as $\Pi^{\rm Phys}(p,p')$. Having denoted by $\Pi^{\rm OPE}(p^2,p'^2,q^2)$ the corresponding invariant amplitude, equated the double Borel transformations $\mathcal{B}\Pi^{\rm OPE}(p^2,p'^2,q^2)$ and $\mathcal{B}\Pi^{\rm Phys}(p^2,p'^2,q^2)$, and performed continuum subtraction, we find the sum rule for the strong coupling $G(q^2)$.

The amplitude $\Pi^{\rm OPE}(p^2,p'^2,q^2)$ after the Borel transformation and continuum subtraction procedures can be expressed using the spectral density $\rho(s,s',q^2)$, which is proportional to a relevant imaginary part of $\Pi^{\rm OPE}(p,p')$:

$$\Pi(\mathbf{M}^2,\mathbf{s}_0,q^2) = \int_{4\mathcal{M}^2}^{s_0} ds\int_{\mathcal{M}^2}^{s_0'} ds'\rho(s,s',q^2) \times e^{-s/M_1^2}e^{-s'/M_2^2}. \tag{26}$$

The Borel and continuum threshold parameters are denoted in Eq. (26) by $\mathbf{M}^2=(M_1^2,M_2^2)$ and $\mathbf{s}_0=(s_0,s_0')$, respectively. Then, the sum rule for $G(q^2)$ reads

$$G(q^2) = \frac{2(m_c+m_s)^2}{m_{D_s}^4 f_{D_s}^2 fm}\frac{q^2-m_{D_s}^2}{m^2+m_{D_s}^2-q^2} \times e^{m^2/M_1^2}e^{m_{D_s}^2/M_2^2}\Pi(\mathbf{M}^2,\mathbf{s}_0,q^2). \tag{27}$$

The coupling $G(q^2)$ is also a function of the Borel and continuum threshold parameters, which, for the sake of simplicity, are not shown in Eq. (27). In what follows, we introduce a variable $Q^2=-q^2$ and label the obtained function $G(Q^2)$.

Equation (27) contains the spectroscopic parameters of the tetraquark X, and the masses and decay constants of the mesons $D_s^{\pm}$. These parameters are input information for our numerical computations: Their values are collected in Table I, which also contains parameters of the mesons η_c, η', and η appearing at the final stages of the other processes. For the masses of the mesons and decay constant f_{D_s}, we use information from Ref. [31]. As the decay constant of the meson η_c, we employ the sum rule's prediction from Ref. [32].

For numerical calculations of $G(Q^2)$, one has to fix working windows for the Borel and continuum subtraction parameters $\mathbf{M}^2$ and $\mathbf{s}_0$. The constraints imposed on

TABLE I. Masses and decay constants of the mesons $D_s^{\pm}$, η_c, η', and η which are employed in numerical calculations.

Quantity	Value (in MeV units)
m_{D_s}	1969.0 ± 1.4
m_{η_c}	2983.9 ± 0.4
$m_{\eta'}$	957.78 ± 0.06
m_{η}	547.862 ± 0.017
f_{D_s}	249.9 ± 0.5
f_{η_c}	320 ± 40

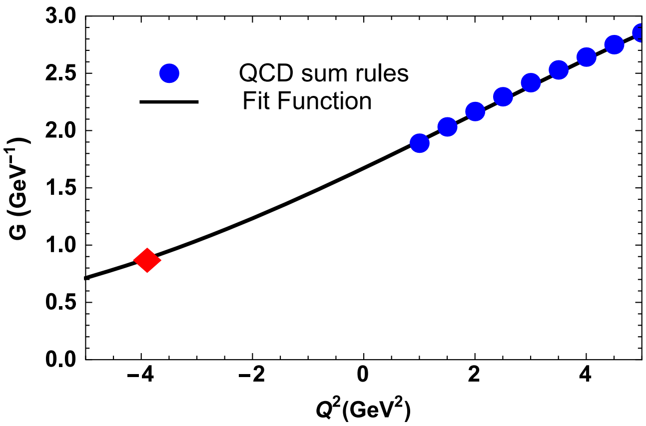

FIG. 4. The sum rule predictions and fit function for the strong coupling $G(Q^2)$. The point $Q^2 = -m_{D_s}^2$ is shown by the red diamond.

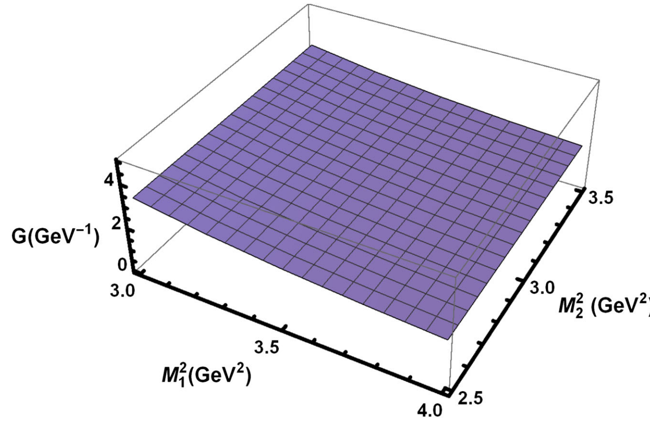

FIG. 5. The strong coupling $G = G(3\ \mathrm{GeV}^2)$ as a function of the Borel parameters M_1^2 and M_2^2 at $s_0 = 21.5\ \mathrm{GeV}^2$ and $s_0' = 5.5\ \mathrm{GeV}^2$.

$\mathbf{M}^2$ and $\mathbf{s}_0$ are usual for sum rule calculations: They have been discussed and explained in Sec. II. The regions for M_1^2 and s_0, that correspond to the X channel, are chosen as in Eq. (15). The parameters (M_2^2, s_0') for the D_s^+ meson channel are varied within the limits

$$M_2^2 \in [2.5, 3.5]\ \mathrm{GeV}^2, \qquad s_0' \in [5, 6]\ \mathrm{GeV}^2. \tag{28}$$

The windows in Eq. (28) are well correlated with the D_s^+ meson's mass. In fact, $\sqrt{s_0'} \approx (m_{D_s} + 0.35)$ GeV is a typical choice for mesons with experimentally measured masses. The Borel parameter M_2 is also comparable with the mass of the D_s^+ meson. The regions in Eq. (28) are numerically very close to the ones given in our article (Ref. [33]) for the D^{*+} channel in the decay $M_{cc}^+ \to D^0 D^{*+}$. Nevertheless, a decisive factor in the choice of (M_2^2, s_0') is fulfillment of the sum rule constraints.

Thus, we calculate $G(Q^2)$ at fixed $Q^2 = 1$–$5\ \mathrm{GeV}^2$ and depict the obtained results in Fig. 4. Let us emphasize that the constraints imposed on the parameters $\mathbf{M}^2$ and $\mathbf{s}_0$ by the sum rule analysis are satisfied at each Q^2. For instance, in Fig. 5, the coupling $G(Q^2)$ is plotted as a function of the parameters M_1^2 and M_2^2 at $Q^2 = 3\ \mathrm{GeV}^2$ in the middle of the s_0 and s_0' regions. Variations of $G(3\ \mathrm{GeV}^2)$ while changing M_1^2 and M_2^2 in explored regions stay within acceptable limits and do not exceed $\pm 25\%$ of the central value. Numerically, we find

$$G(3\ \mathrm{GeV}^2) = (2.53 \pm 0.62)\ \mathrm{GeV}^{-1}. \tag{29}$$

The partial width of the process $X \to D_s^+ D_s^-$ should be calculated in terms of the strong coupling $G(-m_{D_s}^2)$, which is defined at the mass shell $q^2 = m_{D_s}^2$ of the meson D_s^-. But the region $Q^2 < 0$ is not accessible for the sum rule analysis. To solve this problem, it is convenient to introduce a fit function $\mathcal{G}_1(Q^2)$, which for the momenta $Q^2 > 0$ is consistent with predictions of the sum rule computations, but can be extrapolated to the region $Q^2 < 0$. For these purposes, we apply the function $\mathcal{G}_i(Q^2)$, $i = 0, 1, 2$:

$$\mathcal{G}_i(Q^2) = \mathcal{G}_i^0 \exp\left[c_i^1 \frac{Q^2}{m^2} + c_i^2 \left(\frac{Q^2}{m^2}\right)^2\right], \tag{30}$$

where $\mathcal{G}_i^0$, c_i^1, and c_i^2 are parameters, which will be extracted from fitting procedures. Numerical calculations demonstrate that $\mathcal{G}_0^0 = 1.67\ \mathrm{GeV}^{-1}$, $c_0^1 = 2.19$, and $c_0^2 = -1.59$ generate a nice agreement with the sum rule's data shown in Fig. 4.

At the mass shell $q^2 = m_{D_s}^2$, this function predicts

$$G \equiv \mathcal{G}_0(-m_{D_s}^2) = (8.9 \pm 2.2) \times 10^{-1}\ \mathrm{GeV}^{-1}. \tag{31}$$

The width of the process $X \to D_s^+ D_s^-$ is determined by the following formula:

$$\Gamma[X \to D_s^+ D_s^-] = G^2 \frac{m_{D_s}^2 \lambda}{8\pi} \left(1 + \frac{\lambda^2}{m_{D_s}^2}\right), \tag{32}$$

where $\lambda = \lambda(m, m_{D_s}, m_{D_s})$ and

$$\lambda(a, b, c) = \frac{1}{2a}[a^4 + b^4 + c^4 - 2(a^2b^2 + a^2c^2 + b^2c^2)]^{1/2}. \tag{33}$$

Employing the coupling from Eq. (31), it is easy to find the partial width of the process $X \to D_s^+ D_s^-$:

$$\Gamma[X \to D_s^+ D_s^-] = (34.0 \pm 11.9)\ \mathrm{MeV}. \tag{34}$$

IV. PROCESSES $X \to \eta_c\eta'$ AND $X \to \eta_c\eta$

The processes $X \to \eta_c\eta'$ and $X \to \eta_c\eta$, in general, can be studied by a manner described above. However, it is well known that due to $U(1)$ anomaly, there is a mixing in the system of $\eta - \eta'$ mesons [34]. This phenomenon leads to some subtleties in the choice of the interpolating currents for these particles. The $\eta - \eta'$ mixing can be described in the framework of different approaches: The physical particles η and η' can be expressed using either the octet-singlet or quark-flavor bases of the flavor $SU_f(3)$ group. It turns out that mixing of the physical states, decay constants, and higher twist distribution amplitudes in the $\eta - \eta'$ system take simple forms in the quark-flavor basis $|\eta_q\rangle = (\bar{u}u + \bar{d}d)/\sqrt{2}$ and $|\eta_s\rangle = \bar{s}s$ [34–36]. Therefore, for our purposes it is convenient to describe the mesons η and η' in the quark-flavor basis.

Then, the physical mesons η and η' are expressed using the basic states $|\eta_q\rangle$ and $|\eta_s\rangle$:

$$\begin{pmatrix} \eta \\ \eta' \end{pmatrix} = U(\varphi)\begin{pmatrix} |\eta_q\rangle \\ |\eta_s\rangle \end{pmatrix}, \tag{35}$$

where

$$U(\varphi) = \begin{pmatrix} \cos\varphi & -\sin\varphi \\ \sin\varphi & \cos\varphi \end{pmatrix} \tag{36}$$

is the mixing matrix in the $|\eta_q\rangle - |\eta_s\rangle$ basis, with φ being a mixing angle. This assumption on the state mixing implies that the same pattern applies to relevant currents, decay constants, and wave functions as well.

In this context, the interpolating currents for the mesons η and η' are given by the expressions

$$J^{\eta}(x) = -\sin\varphi\bar{s}_j(x)i\gamma_5 s_j(x),$$
$$J^{\eta'}(x) = \cos\varphi\bar{s}_j(x)i\gamma_5 s_j(x), \tag{37}$$

where j is the color index. Let us emphasize that in Eq. (37), we write down only the $\bar{s}s$ component of the currents, which contribute to the decays under analysis.

We begin our calculations from the decay $X \to \eta_c\eta'$. In this case, one should explore the correlation function

$$\tilde{\Pi}(p,p') = i^2\int d^4x d^4y e^{i(p'y-px)}\langle 0|\mathcal{T}\{J^{\eta_c}(y) \times J^{\eta'}(0)J^{\dagger}(x)\}|0\rangle, \tag{38}$$

with $J^{\eta_c}(y)$ being the interpolating current of the meson η_c:

$$J^{\eta_c}(x) = \bar{c}_i(x)i\gamma_5 c_i(x). \tag{39}$$

The ground-state contribution to the correlation function $\tilde{\Pi}(p,p')$ in terms of the involved particles' matrix elements has the form

$$\tilde{\Pi}^{\rm Phys}(p,p') = \frac{\langle 0|J^{\eta_c}|\eta_c(p')\rangle\langle 0|J^{\eta'}|\eta'(q)\rangle}{(p^2-m^2)(p'^2-m_{\eta_c}^2)} \times \frac{\langle \eta'(q)\eta_c(p')|X(p)\rangle\langle X(p)|J^{\dagger}|0\rangle}{(q^2-m_{\eta'}^2)} + \cdots, \tag{40}$$

where the dots indicate the effects of higher resonances and continuum states. The function $\tilde{\Pi}^{\rm Phys}(p,p')$ can be simplified by invoking the matrix elements of the mesons η_c and η':

$$\langle 0|J^{\eta_c}|\eta_c\rangle = \frac{m_{\eta_c}^2 f_{\eta_c}}{2m_c},$$
$$2m_s\langle \eta'|\bar{s}i\gamma_5 s|0\rangle = h_{\eta'}^s, \tag{41}$$

where m_{η_c} and f_{η_c} are the mass and decay constant of the η_c meson. The twist-3 matrix element of the local operator $\bar{s}i\gamma_5 s$ sandwiched between the meson η' and vacuum states is denoted by $h_{\eta'}^s$ [35]. The parameter $h_{\eta'}^s$ complies with the mixing effect, and we get

$$h_{\eta'}^s = h_s\cos\varphi. \tag{42}$$

The parameter h_s in Eq. (42) can be defined theoretically [35], but for our analysis it is enough to use phenomenological values of h_s and φ:

$$h_s = (0.087 \pm 0.006)\ \text{GeV}^3,$$
$$\varphi = 39.3° \pm 1.0°. \tag{43}$$

The vertex $X\eta_c\eta'$ is chosen in the following form:

$$\langle \eta'(q)\eta_c(p')|X(p)\rangle = g_1(q^2)p\cdot p', \tag{44}$$

where g_1 is the strong coupling corresponding to the vertex $X\eta_c\eta'$. Using these matrix elements, one can obtain a new expression for $\Pi^{\rm Phys}(p,p')$:

$$\tilde{\Pi}^{\rm Phys}(p,p') = g_1(q^2)\frac{fmm_{\eta_c}^2 f_{\eta_c} h_s\cos^2\varphi}{4m_c m_s(p^2-m^2)} \times \frac{1}{(p'^2-m_{\eta_c}^2)(q^2-m_{\eta'}^2)} \times \frac{m^2+m_{\eta_c}^2-q^2}{2} + \cdots. \tag{45}$$

The QCD side of the sum rule for $g_1(q^2)$ is given by the formula

$$\tilde{\Pi}^{\rm OPE}(p,p') = -\cos\varphi \int d^4x d^4y e^{i(p'y-px)}\epsilon\tilde{\epsilon} \times {\rm Tr}[\gamma_5 S_c^{ib}(y-x)\gamma_5 \tilde{S}_s^{jc}(-x)\gamma_5 \tilde{S}_s^{nj}(x) \times \gamma_5 S_c^{mi}(x-y)]. \quad (46)$$

The sum rule for the coupling $g_1(q^2)$ is derived using Borel transformations of invariant amplitudes $\tilde{\Pi}^{\rm Phys}(p^2,p'^2,q^2)$ and $\tilde{\Pi}^{\rm OPE}(p^2,p'^2,q^2)$ and reads

$$g_1(q^2) = -\frac{8m_c m_s}{fm m_{\eta_c}^2 f_{\eta_c} h_s \cos\varphi} \frac{q^2-m_{\eta_c}^2}{m^2+m_{\eta_c}^2-q^2} \times e^{m^2/M_1^2} e^{m_{\eta_c}^2/M_2^2} \tilde{\Pi}(\mathbf{M}^2,\mathbf{s}_0,q^2). \quad (47)$$

Here, $\tilde{\Pi}(\mathbf{M}^2,\mathbf{s}_0,q^2)$ is the Borel transformed and subtracted amplitude $\tilde{\Pi}^{\rm OPE}(p^2,p'^2,q^2)$.

The coupling $g_1(q^2)$ is calculated using the following Borel and continuum threshold parameters in the η_c channel:

$$M_2^2 \in [3,4]\ {\rm GeV}^2, \qquad s_0' \in [9.5,10.5]\ {\rm GeV}^2, \quad (48)$$

whereas with M_1^2 and s_0 for the X channel, we employ Eq. (15). The strong coupling g_1 is defined at the mass shell of the η' meson. The fit function $\mathcal{G}_1(Q^2)$ given by Eq. (30) has the parameters $\mathcal{G}_1^0 = 0.26\ {\rm GeV}^{-1}$, $c_1^1 = 4.72$, and $c_1^2 = -3.52$. Relevant computations yield

$$g_1 \equiv \mathcal{G}_1(-m_{\eta'}^2) = (1.9 \pm 0.3) \times 10^{-1}\ {\rm GeV}^{-1}. \quad (49)$$

The partial width of this decay can be found by means of the formula Eq. (32), in which one should make the substitutions $G \to g_1$, $m_{D_s}^2 \to m_{\eta_c}^2$, and $\lambda(m, m_{D_s}, m_{D_s}) \to \tilde{\lambda}(m, m_{\eta_c}, m_{\eta'})$. Then, for the process $X \to \eta_c\eta'$, we get

$$\Gamma[X \to \eta_c\eta'] = (3.0 \pm 0.7)\ {\rm MeV}. \quad (50)$$

Analysis of the decay $X \to \eta_c\eta$ can be performed in a similar way. Omitting further details, let us write down predictions obtained for key quantities. Thus, the strong coupling g_2 at the vertex $X\eta_c\eta$ is determined by the equality

$$g_2 \equiv |\mathcal{G}_2(-m_\eta^2)| = (1.4 \pm 0.2) \times 10^{-1}\ {\rm GeV}^{-1}, \quad (51)$$

where parameters of the fit function are $\mathcal{G}_2^0 = -0.15\ {\rm GeV}^{-1}$, $c_2^1 = 5.76$, and $c_2^2 = -4.44$. The partial width of the decay $X \to \eta_c\eta$ is

$$\Gamma[X \to \eta_c\eta] = (5.2 \pm 1.1)\ {\rm MeV}. \quad (52)$$

With this information in hand, it is not difficult to find the full width of the scalar tetraquark X:

$$\Gamma_{\rm X} = (42.2 \pm 12.0)\ {\rm MeV}. \quad (53)$$

This estimate is in excellent agreement with the LHCb data.

V. CONCLUDING NOTES

In this article, we have calculated spectral parameters of the scalar tetraquark X in the framework of the QCD two-point sum rule method. We evaluated also the full width of X by taking into account its decay modes $X \to D_s^+ D_s^-$, $X \to \eta_c\eta'$, and $X \to \eta_c\eta$. Our result for the mass $m = (3976 \pm 85)$ MeV of the tetraquark X overshoots the corresponding LHCb datum, but it is compatible with $m_{\rm exp}$, provided one takes into account the corresponding theoretical and experimental errors. Our prediction for the full width $\Gamma_{\rm X} = (42.2 \pm 12.0)$ MeV of X is in excellent agreement with $\Gamma_{\rm exp}$ from Eq. (1).

In Ref. [1], the LHCb Collaboration assumed that the resonance $X(3960)$ is composed of four $c\bar{c}s\bar{s}$ quarks. This assumption relies on theoretical predictions of Ref. [10], in which the authors used the QCD sum rule method and different interpolating currents to find the mass spectra of the diquark-antidiquark states $qc\bar{q}\bar{c}$ and $sc\bar{s}\bar{c}$ with $J^{\rm PC} = 0^{++}$ and 2^{++}. Some of the currents used there indeed led to estimations which are comparable with $m_{\rm exp}$ if one takes into consideration the ambiguities of the analysis.

In the context of the sum rule approach, $X(3960)$ was modeled as a $D_s^+ D_s^-$ molecule state [18], as well. In accordance with this paper, the mass of such a hadronic molecule is equal to (3980 ± 100) MeV, being in agreement with the LHCb data. It is worth noting that in Refs. [10,18], the authors did not investigate quantitatively the widths of the diquark-antidiquark or molecule states considered there, which is crucial for drawing a conclusion about the inner organization of $X(3960)$.

The results for m and $\Gamma_{\rm X}$ obtained in the present article allow us to consider $X(3960)$ as a candidate to a scalar diquark-antidiquark exotic meson. At the same time, a molecule model for $X(3960)$ should be studied in a more detailed form: There is a necessity to evaluate the full width of a molecule state. Only after such comprehensive analysis will it be possible to make a choice between the competing models.

APPENDIX: THE PROPAGATORS $S_{q(Q)}(x)$ AND THE INVARIANT AMPLITUDE $\Pi(M^2, s_0)$

In the current article, for the light quark propagator $S_q^{ab}(x)$, we employ the following expression:

$$S_q^{ab}(x) = i\delta_{ab}\frac{\not x}{2\pi^2 x^4} - \delta_{ab}\frac{m_q}{4\pi^2 x^2} - \delta_{ab}\frac{\langle \bar{q}q\rangle}{12} + i\delta_{ab}\frac{\not x m_q \langle \bar{q}q\rangle}{48} - \delta_{ab}\frac{x^2}{192}\langle \bar{q}g_s\sigma Gq\rangle + i\delta_{ab}\frac{x^2 \not x m_q}{1152}\langle \bar{q}g_s\sigma Gq\rangle$$
$$- i\frac{g_s G_{ab}^{\alpha\beta}}{32\pi^2 x^2}[\not x\sigma_{\alpha\beta} + \sigma_{\alpha\beta}\not x] - i\delta_{ab}\frac{x^2 \not x g_s^2 \langle \bar{q}q\rangle^2}{7776} - \delta_{ab}\frac{x^4 \langle \bar{q}q\rangle\langle g_s^2 G^2\rangle}{27648} + \cdots. \tag{A1}$$

For the heavy quark $Q = c$, we use the propagator $S_Q^{ab}(x)$:

$$S_Q^{ab}(x) = i\int \frac{d^4k}{(2\pi)^4} e^{-ikx}\left\{\frac{\delta_{ab}(\not k + m_Q)}{k^2 - m_Q^2} - \frac{g_s G_{ab}^{\alpha\beta}}{4}\frac{\sigma_{\alpha\beta}(\not k + m_Q) + (\not k + m_Q)\sigma_{\alpha\beta}}{(k^2 - m_Q^2)^2}\right.$$
$$\left. + \frac{g_s^2 G^2}{12}\delta_{ab} m_Q \frac{k^2 + m_Q \not k}{(k^2 - m_Q^2)^4} + \frac{g_s^3 G^3}{48}\delta_{ab}\frac{(\not k + m_Q)}{(k^2 - m_Q^2)^6}[\not k(k^2 - 3m_Q^2) + 2m_Q(2k^2 - m_Q^2)](\not k + m_Q) + \cdots\right\}. \tag{A2}$$

Here, we have used the shorthand notations

$$G_{ab}^{\alpha\beta} \equiv G_A^{\alpha\beta}\lambda_{ab}^A/2, \qquad G^2 = G_{\alpha\beta}^A G_A^{\alpha\beta}, \qquad G^3 = f^{ABC} G_{\alpha\beta}^A G^{B\beta\delta} G_\delta^{C\alpha}, \tag{A3}$$

where $G_A^{\alpha\beta}$ is the gluon field strength tensor, while λ^A and f^{ABC} are the Gell-Mann matrices and structure constants of the color group $SU_c(3)$, respectively. The indices A, B, C run in the range $1, 2, \ldots 8$.

The invariant amplitude $\Pi(M^2, s_0)$ obtained after the Borel transformation and subtraction procedures is given by Eq. (9):

$$\Pi(M^2, s_0) = \int_{4\mathcal{M}^2}^{s_0} ds \rho^{\mathrm{OPE}}(s) e^{-s/M^2} + \Pi(M^2),$$

where the spectral density $\rho^{\mathrm{OPE}}(s)$ and the function $\Pi(M^2)$ are determined by the expressions

$$\rho^{\mathrm{OPE}}(s) = \rho^{\mathrm{pert.}}(s) + \sum_{N=3}^{8}\rho^{\mathrm{DimN}}(s), \qquad \Pi(M^2) = \sum_{N=6}^{10}\Pi^{\mathrm{DimN}}(M^2), \tag{A4}$$

respectively. The components of $\rho^{\mathrm{OPE}}(s)$ and $\Pi(M^2)$ are given by the formulas

$$\rho^{\mathrm{DimN}}(s) = \int_0^1 d\alpha \int_0^{1-a} d\beta \rho^{\mathrm{DimN}}(s, \alpha, \beta), \qquad \rho^{\mathrm{DimN}}(s) = \int_0^1 d\alpha \rho^{\mathrm{DimN}}(s, \alpha), \tag{A5}$$

and

$$\Pi^{\mathrm{DimN}}(M^2) = \int_0^1 d\alpha \int_0^{1-a} d\beta \Pi^{\mathrm{DimN}}(M^2, \alpha, \beta), \qquad \Pi^{\mathrm{DimN}}(M^2) = \int_0^1 d\alpha \Pi^{\mathrm{DimN}}(M^2, \alpha). \tag{A6}$$

In Eqs. (A5) and (A6), variables α and β are Feynman parameters.

The perturbative and nonperturbative components of the spectral density $\rho^{\mathrm{pert.}}(s, \alpha, \beta)$ and $\rho^{\mathrm{Dim3(4,5,6,7,8)}}(s, \alpha, \beta)$ have the forms

$$\rho^{\mathrm{pert.}}(s, \alpha, \beta) = \frac{\Theta(L)L^2}{512\pi^6(\beta - 1)^4 N_1^4 N_2}\{2(\beta - 1)^2 N_3[-\alpha\beta N_3 + 3m_c m_s(\alpha + \beta)N_1^2]$$
$$+4(\beta - 1)N_1^2 L[-\alpha\beta N_3 + m_c m_s(\alpha + \beta)N_1^2] - \alpha\beta N_1^4 L^2\}, \tag{A7}$$

$$\rho^{\mathrm{Dim3}}(s, \alpha, \beta) = -\frac{\langle \bar{s}s\rangle\Theta(L)}{16\pi^4(\beta - 1)^2 N_1^6}\{m_s(\beta - 1)^2\alpha\beta N_2 N_3^2 + (\beta - 1)N_1^2[6m_s\alpha\beta N_2 N_3 + 2m_c^2 m_s N_1^3$$
$$- m_c s\alpha\beta L(\beta^4 + \alpha^2(\alpha - 1)^2 + \beta^3(3\alpha - 2) + \alpha\beta(2 - 5\alpha + 3\alpha^2) + \beta^2(1 - 5\alpha + 4\alpha^2))]$$
$$- N_1^4[-3m_s\alpha\beta N_2 + m_c L^2(\beta^3 + 2\beta\alpha(\alpha - 1) + \alpha^2(\alpha - 1) + \beta^2(2\alpha - 1)]\}, \tag{A8}$$

$$\rho^{\mathrm{Dim4}}(s,\alpha,\beta)=\frac{\langle\alpha_sG^2/\pi\rangle\Theta(L)}{4608\pi^4(\beta-1)^2N_1^5N_2^2}\{\alpha\beta(\beta-1)^2[-6m_cm_s(\beta^3+\beta^2(\alpha-1)+\beta^2\alpha+\alpha^2(\alpha-1))$$
$$\times(3N_2N_3+2m_c^2N_1)+N_2N_3(\alpha+\beta)(54N_2N_3+m_c^2(\beta^4-\beta^3+\beta^2\alpha^2+\alpha^3(\alpha-1))/N_1$$
$$+sm_cN_2^2(11m_c\alpha\beta(\alpha^3+\beta^3)+6m_s(2\beta^5-73\beta^3\alpha(\alpha-1)+2\alpha^4(\alpha-1)-\beta^4(2+37\alpha)+\beta^2\alpha$$
$$\times(-36+108\alpha-73\alpha^2)+\beta\alpha^2(-36+73\alpha-37\alpha^2)))]+12N_1^2(\beta-1)L[27N_2^2N_3\alpha\beta(\alpha+\beta)/N_1$$
$$+m_c^2\alpha\beta(\alpha^3+\beta^3)N_2+m_cm_s(2\beta^6+2\alpha^4(\alpha-1)^2-\beta^5(4+35\alpha)+\beta^3\alpha(-109+254\alpha-146\alpha^2)$$
$$+\beta^4(2+108\alpha-110\alpha^2)+\beta\alpha^2(36-109\alpha+108\alpha^2-35\alpha^3)-2\beta^2\alpha(-18+90\alpha-127\alpha^2+55\alpha^3))]$$
$$+162L^2\alpha\beta N_1^3N_2(\beta^2+\alpha(\alpha-1)+\beta(2\alpha-1))\},\tag{A9}$$

$$\rho^{\mathrm{Dim5}}(s,\alpha,\beta)=\frac{\langle\bar{s}g_s\sigma Gs\rangle\alpha\beta N_2\Theta(L)}{64\pi^4(\beta-1)N_1^6}\{(\beta-1)[13m_s\alpha\beta N_2N_3+4m_c^2m_sN_1^3-6m_cs\alpha\beta(\beta^4$$
$$+\alpha^2(\alpha-1)^2+\beta^3(3\alpha-2)+\beta\alpha(2-5\alpha+3\alpha^2)+\beta^2(1-5\alpha+4\alpha^2))]-2N_1^2L[-8m_s\alpha\beta N_2$$
$$+3m_c(\beta^3+2\beta\alpha(\alpha-1)+\alpha^2(\alpha-1)+\beta^2(2\alpha-1))]\},\tag{A10}$$

$$\rho^{\mathrm{Dim6}}(s,\alpha,\beta)=\frac{\Theta(L)}{829440\pi^6(\beta-1)^2N_1^5N_2^2}\{3840g_s^2\langle\bar{s}s\rangle^2\pi^2(\beta-1)\alpha\beta N_2^4[s(\beta-1)\alpha\beta N_2+N_1^2L]$$
$$-27\langle g_s^3G^3\rangle m_c^2\beta^5(\beta-1)^2[2(\beta-1)\beta\alpha N_2-2\alpha(-5\beta^3+\beta^2(10-3\alpha)+2\alpha(\alpha-1)^2$$
$$+\beta(-5+\alpha+4\alpha^2))]\},\tag{A11}$$

$$\rho_1^{\mathrm{Dim7}}(s,\alpha,\beta)=\frac{\langle\alpha_sG^2/\pi\rangle\langle\bar{s}s\rangle\Theta(L)}{1152\pi^2(\beta-1)N_1^4}\{90m_s(\beta-1)\alpha\beta(\alpha+\beta)N_2^2+18m_s(\beta-1)\alpha\beta N_2$$
$$\times[\beta^2+\alpha(\alpha-1)+\beta(2\alpha-1)]+8m_c[2\beta^6+2\alpha^4(\alpha-1)^2-\beta^5(4+19\alpha)+\beta^4(2+56\alpha-37\alpha^2)$$
$$+\beta^3\alpha(-55+91\alpha-37\alpha^2)+\beta^2\alpha(18-72\alpha+74\alpha^2-17\alpha^3)+\beta\alpha^2(18-37\alpha+15\alpha^2+4\alpha^3)]\},\tag{A12}$$

$$\rho^{\mathrm{Dim8}}(s,\alpha,\beta)=-\frac{\langle\alpha_sG^2/\pi\rangle^2\alpha^2\beta^2N_2\Theta(L)}{512\pi^2N_1^4}.\tag{A13}$$

The function $\rho_2^{\mathrm{Dim7}}(s,\alpha)$ is determined by the expression

$$\rho_2^{\mathrm{Dim7}}(s,\alpha)=-\frac{\langle\alpha_sG^2/\pi\rangle\langle\bar{s}s\rangle m_c}{288\pi^2}\Theta(\tilde{L}).\tag{A14}$$

Components of $\Pi(M^2)$ are

$$\Pi^{\mathrm{Dim6}}(M^2,\alpha,\beta)=\frac{\langle g_s^3G^3\rangle m_c^3\beta^4(\beta-1)}{92160M^4\pi^6N_1^6N_2}\exp\left[-\frac{m_c^2(\alpha+\beta)N_1}{M^2\alpha\beta N_2}\right]\{-[2m_c^5\alpha\beta(\beta-1)^2(\alpha+\beta)^2$$
$$+3m_cM^4\alpha\beta N_1^2][3\beta^3+\beta\alpha(\alpha-2)-\alpha^2(\alpha-1)+\beta^2(2\alpha-3)]+6m_sM^4N_1^3[8\beta^3+\beta\alpha(\alpha-3)$$
$$+\alpha^2(\alpha-1)+\beta^2(3\alpha-8)]+6m_c^2m_sM^2(\beta-1)N_1^2[8\beta^4+2\beta\alpha^2(\alpha-2)+\alpha^3(\alpha-1)$$
$$+\beta^2\alpha(4\alpha-11)+\beta^3(11\alpha-8)]+6m_c^4m_s(\beta-1)^2[2\beta^7-\alpha^5(\alpha-1)^2+\beta^6(5\alpha-4)$$
$$+\beta^3\alpha^2(2+11\alpha-14\alpha^2)+\beta^4\alpha(5-4\alpha-7\alpha^2)+\beta\alpha^4(-4+9\alpha-5\alpha^2)+2\beta^5(1-5\alpha+\alpha^2)$$
$$-4\beta^2\alpha^3(1-4\alpha+3\alpha^2)]+3m_c^3M^2\alpha\beta(\beta-1)[3\beta^6-\beta\alpha^4(\alpha-1)-\alpha^4(\alpha-1)^2+\beta^5(8\alpha-6)$$
$$+2\beta^2\alpha^2(3-4\alpha+\alpha^2)+\beta^3\alpha(8-17\alpha+8\alpha^2)+\beta^4(3-16\alpha+11\alpha^2)]\},\tag{A15}$$

$$\Pi^{\text{Dim7}}(M^2,\alpha,\beta)=\frac{\langle\alpha_s G^2/\pi\rangle\langle\bar{s}s\rangle m_c^2}{576\pi^2 M^4 N_1^7}\exp\left[-\frac{m_c^2(\alpha+\beta)N_1}{M^2\alpha\beta N_2}\right]\{-2m_c M^2\alpha\beta(\beta-1)[m_c^2(\alpha+\beta)(\beta-1)$$
$$+M^2N_1][2\beta^6+2\alpha^4(\alpha-1)^2+\beta^5(5\alpha-4)+\beta\alpha^3(4-9\alpha+5\alpha^2)+\alpha^2\beta^2(4-13\alpha+9\alpha^2)$$
$$+\beta^4(2-9\alpha+9\alpha^2)+\beta^3\alpha(4-13\alpha+10\alpha^2)]+m_s[2m_c^4(\beta-1)^3\alpha\beta(\alpha+\beta)^3(\beta^3-\beta^2+\beta\alpha+\alpha^2(\alpha-1))$$
$$+m_c^2M^2(\beta-1)^2\alpha\beta(\alpha+\beta)^2(7\beta^5+3\beta^4(5\alpha-6)+\alpha^2(\alpha-1)^2(7\alpha-4)+\beta^3(15-35\alpha+23\alpha^2)$$
$$+\alpha\beta(-8+28\alpha-35\alpha^2+15\alpha^3)+\beta^2(-4+28\alpha-47\alpha^2+23\alpha^3))-M^4N_1^2(8\beta^7+8\alpha^4(\alpha-1)^3$$
$$+3\beta^6(3\alpha-8)+\beta^5(24-30\alpha+17\alpha^2)+3\beta\alpha^3(-4+15\alpha-19\alpha^2+8\alpha^3)+3\beta^3\alpha(-4+12\alpha-20\alpha^2+11\alpha^3)$$
$$+\beta^4(-8+33\alpha-45\alpha^2+24\alpha^3)+\beta^2\alpha^2(-8+48\alpha-70\alpha^2+33\alpha^3))]\}, \tag{A16}$$

$$\Pi^{\text{Dim8}}(M^2,\alpha,\beta)=-\frac{\langle\alpha_s G^2/\pi\rangle^2\alpha\beta(\beta-1)}{82944\pi^2M^6N_1^8N_2}\exp\left[-\frac{m_c^2(\alpha+\beta)N_1}{M^2\alpha\beta N_2}\right]\{2m_c^7(\beta-1)^3\alpha^3\beta^3(\alpha+\beta)^2$$
$$-6m_c^6m_s(\beta-1)^3\alpha^2\beta^2(\alpha+\beta)^3N_2+81m_cM^6\alpha\beta N_1^3[\beta^3+\beta^2(\alpha-1)+\beta\alpha^2+\alpha^2(\alpha-1)]+216m_sM^6N_1^3$$
$$\times[\beta^5+\beta^4(\alpha-2)-\beta^3(\alpha-1)+\beta\alpha^3(\alpha-1)+\alpha^3(\alpha-1)^2]+81m_c^3M^4(\beta-1)\alpha\beta N_1^2[\beta^4+\alpha^3(\alpha-1)$$
$$+\beta^3(2\alpha-1)+\beta^2\alpha(2\alpha-1)+\beta\alpha^2(2\alpha-1)]+216m_c^2m_sM^4(\beta-1)N_1^2[\beta^6+2\beta^5(\alpha-1)-\beta^3\alpha(\alpha-1)$$
$$+\beta^2\alpha^3(\alpha-1)+\alpha^4(\alpha-1)^2+\beta^4(1-3\alpha+\alpha^2)+\beta\alpha^3(1-3\alpha+2\alpha^2)]+54m_c^5M^2(\beta-1)^2\alpha\beta(\alpha+\beta)^2$$
$$\times[\beta^5+2\beta^4(\alpha-1)+\alpha^3(\alpha-1)+\beta\alpha^2(1-3\alpha+2\alpha^2)+\beta^2\alpha(1-4\alpha+3\alpha^2)+\beta^3(1-3\alpha+3\alpha^2]$$
$$-12m_c^4m_sM^2(\beta-1)^2\alpha\beta[9\beta^7+9\alpha^4(\alpha-1)^3+4\beta\alpha^3(\alpha-1)(13\alpha-9)+\beta^6(52\alpha-27)+\beta^5(27-140\alpha$$
$$+138\alpha^2)+3\beta^2\alpha^2(-18+79\alpha-107\alpha^2+46\alpha^3)+\beta^3\alpha(-36+237\alpha-416\alpha^2+215\alpha^3)$$
$$+\beta^4(-9+124\alpha-321\alpha^2+215\alpha^3)]\}. \tag{A17}$$

The terms Dim9 and Dim10 are exclusively of the type in Eq. (A6) and have the two components $\Pi_1^{\text{DimN}}(M^2,\alpha,\beta)$ and $\Pi_2^{\text{DimN}}(M^2,\alpha)$ presented below:

$$\Pi_1^{\text{Dim9}}(M^2,\alpha,\beta)=\frac{m_c(\beta-1)}{17280\pi^4M^8N_1^{10}}\exp\left[-\frac{m_c^2(\alpha+\beta)N_1}{M^2\alpha\beta N_2}\right]\{5\langle\alpha_sG^2/\pi\rangle\langle\bar{s}g_s\sigma Gs\rangle M^2\pi^2N_1^2N_2$$
$$\times[2m_c^5m_s(\beta-1)^3\alpha\beta(\alpha+\beta)^3(\beta^3-\beta^2+\beta\alpha+\alpha^2(\alpha-1))+6M^6N_1^3(\beta^5-\beta^4+\alpha^4(\alpha-1))$$
$$+6m_c^2M^4(\beta-1)N_1^2(\beta^6+\beta^5(\alpha-1)-\beta^4\alpha+\beta\alpha^4(\alpha-1)+\alpha^5(\alpha-1))-3m_c^4M^2(\beta-1)^2\alpha\beta$$
$$\times(2\beta^7+2\alpha^5(\alpha-1)^2+\beta^6(7\alpha-4)+\beta\alpha^4(6-13\alpha+7\alpha^2)+2\beta^2\alpha^3(4-11\alpha+7\alpha^2)$$
$$+\beta^5(2-13\alpha+14\alpha^2)+\beta^3\alpha^2(8-26\alpha+19\alpha^2)+\beta^4\alpha(6-22\alpha+19\alpha^2))]$$
$$+3\langle g_s^3G^3\rangle\langle\bar{s}s\rangle m_c^3(\beta-1)^2[m_cM^4N_1^4(6\beta^6+8\beta^5\alpha+3\beta^4\alpha^2+3\beta^2\alpha^4+8\beta\alpha^5+6\alpha^6)$$
$$-8m_sM^4N_1^4(2\beta^6+3\beta^4\alpha(\alpha-1)+3\beta^2\alpha^4+3\beta\alpha^4(\alpha-1)+2\alpha^5(\alpha-1)+\beta^5(3\alpha-2))$$
$$-m_c^4m_s(\beta-1)^2\alpha\beta(\alpha+\beta)^3(3\beta^7+2\beta^6(\alpha-3)-\beta^3\alpha^3(\alpha-3)+\beta^2\alpha^4(\alpha-1)+3\alpha^5(\alpha-1)^2$$
$$+\beta^5(3-\alpha+\alpha^2)-\beta^4\alpha(1+\alpha+\alpha^2)+\beta\alpha^4(-1-\alpha+2\alpha^2))-m_c^2m_sM^2(\beta-1)N_1^2$$
$$\times(4\beta^9-3\beta\alpha^7(\alpha-1)+4\alpha^7(\alpha-1)^2-\beta^8(8+3\alpha)-3\beta^6\alpha^2(7\alpha-8)+\beta^5\alpha^2(-12+29\alpha-25\alpha^2)$$
$$+\beta^4\alpha^3(-8+32\alpha-25\alpha^2)+\beta^3\alpha^4(-8+29\alpha-21\alpha^2)+\beta^7(4+3\alpha-15\alpha^2)-3\beta^2\alpha^5(4-8\alpha+5\alpha^2))$$
$$+m_c^3M^2(\beta-1)N_1^2(2\beta^9+\beta^5\alpha^3(3-5\alpha)+\beta^4\alpha^4(2-5\alpha)+\beta^3\alpha^5(3-7\alpha)+3\beta\alpha^7(\alpha-1)$$
$$+2\alpha^8(\alpha-1)-3\beta^7\alpha(1+\alpha)+\beta^8(3\alpha-2)+\beta^6\alpha^2(1-7\alpha)+\beta^2\alpha^6(1-3\alpha))]\}, \tag{A18}$$

$$\Pi_2^{\text{Dim9}}(M^2,\alpha)=\frac{\langle\alpha_sG^2/\pi\rangle\langle\bar{s}g_s\sigma Gs\rangle m_c}{1152M^4\pi^2\alpha^4(\alpha-1)^2}\exp\left[-\frac{m_c^2}{M^2\alpha(1-\alpha)}\right][2m_c^3m_s(\alpha-1)$$
$$-9m_c^2M^2\alpha^2(\alpha-1)+9M^4\alpha^3(\alpha-1)^2+4m_cm_sM^2\alpha(1-\alpha-2\alpha^2+3\alpha^3)], \tag{A19}$$

$$\Pi_1^{\mathrm{Dim10}}(M^2,\alpha,\beta) = -\frac{m_c^3\alpha\beta(\beta-1)^3}{3645\times 10^{11}M^{10}\pi^4 N_1^{11}N_2}\exp\left[-\frac{m_c^2(\alpha+\beta)N_1}{M^2\alpha\beta N_2}\right]\{320 g_s^2\langle\bar{s}s\rangle^2\pi^2 m_c^3 M^4$$
$$\times(\beta-1)(\beta^2-\beta\alpha+\alpha^2)[\beta^4+\alpha^2(\alpha-1)^2+\beta^3(3\alpha-2)+\beta\alpha(2-5\alpha+3\alpha^2)+\beta^2(1-5\alpha+4\alpha^2)]^3$$
$$+9\langle g_s^3G^3\rangle\alpha^2\beta^2[12m_c^3M^4\alpha^2\beta^2(\beta-1)N_1^3+18m_sM^6(\alpha+\beta)N_1^5-m_c^7\alpha\beta(\beta-1)^3(\alpha+\beta)^2$$
$$\times(3\beta^4+\beta^3(\alpha-3)+\beta\alpha^2(\alpha-1)+3\alpha^3(\alpha-1)+\beta^2\alpha(2\alpha-1))-6m_c^2m_sM^4(\beta-1)N_1^3(5\beta^4$$
$$+22\beta\alpha^2(\alpha-1)+5\alpha^3(\alpha-1)+2\beta^2\alpha(19\alpha-11)+\beta^3(22\alpha-5))+3m_c^6m_s(\beta-1)^3(\alpha+\beta)^2(5\beta^6$$
$$+3\beta\alpha^4(\alpha-1)+5\alpha^4(\alpha-1)^2+\beta^5(3\alpha-10)-2\beta^3\alpha^2(7\alpha-8)+\beta^4(5-3\alpha-6\alpha^2)-2\alpha^2\beta^2$$
$$\times(5-8\alpha+3\alpha^2))+3m_c^5M^2\alpha\beta(\beta-1)^2(3\beta^7+\beta^4\alpha(5-4\alpha)+4\beta^2\alpha^4(\alpha-1)+5\beta\alpha^4(\alpha-1)^2$$
$$+3\alpha^5(\alpha-1)^2+\beta^6(5\alpha-6)+\beta^5(3-10\alpha+4\alpha^2))-3m_c^4m_sM^2(\beta-1)^2(13\beta^9+13\alpha^6(\alpha-1)^3$$
$$+\beta^8(20\alpha-39)+\beta\alpha^5(\alpha-1)^2(20\alpha-11)-\beta^2\alpha^4(\alpha-1)^2(45\alpha-73)+\beta^7(39-51\alpha-45\alpha^2)$$
$$+\beta^4\alpha^2(73-510\alpha+808\alpha^2-371\alpha^3)+\beta^6(-13+42\alpha+163\alpha^2-211\alpha^3)$$
$$+\beta^3\alpha^3(142-510\alpha+579\alpha^2-211\alpha^3)-\beta^5\alpha(11+191\alpha-579\alpha^2+371\alpha^3))]\}, \tag{A20}$$

and

$$\Pi_2^{\mathrm{Dim10}}(M^2,\alpha) = \frac{\langle\alpha_sG^2/\pi\rangle g_s^2\langle\bar{s}s\rangle^2 m_c^3 m_s}{23328M^4\pi^2(\alpha-1)^3}\exp\left[-\frac{m_c^2}{M^2\alpha(1-\alpha)}\right]. \tag{A21}$$

In the expressions above, $\Theta(x)$ is the Unit Step function. We have also used the following shorthand notations:

$$N_1=\beta^2+(\alpha+\beta)(\alpha-1), \qquad N_2=\alpha+\beta-1, \qquad N_3=s\alpha\beta N_2,$$
$$L\equiv L(s,\alpha,\beta)=\frac{(\beta-1)[N_3-m_c^2(\alpha+\beta)N_1]}{N_1^2}, \qquad \tilde{L}\equiv\tilde{L}(s,\alpha)=s\alpha(1-\alpha)-m_c^2. \tag{A22}$$

[1] The LHCb Collaboration, arXiv:2210.15153.
[2] R. Aaij *et al.* (LHCb Collaboration), Phys. Rev. Lett. **118**, 022003 (2017); Phys. Rev. D **95**, 012002 (2017).
[3] T. Aaltonen *et al.* (CDF Collaboration), Phys. Rev. Lett. **102**, 242002 (2009).
[4] S. Chatrchyan *et al.* (CMS Collaboration), Phys. Lett. B **734**, 261 (2014).
[5] V. M. Abazov *et al.* (D0 Collaboration), Phys. Rev. D **89**, 012004 (2014).
[6] R. Aaij *et al.* (LHCb Collaboration), Phys. Rev. Lett. **127**, 082001 (2021).
[7] J. Nieves and M. P. Valderrama, Phys. Rev. D **86**, 056004 (2012).
[8] Z. G. Wang, Eur. Phys. J. C **74**, 2874 (2014).
[9] R. F. Lebed and A. D. Polosa, Phys. Rev. D **93**, 094024 (2016).
[10] W. Chen, H. X. Chen, X. Liu, T. G. Steele, and S. L. Zhu, Phys. Rev. D **96**, 114017 (2017).
[11] L. Meng, B. Wang, and S. L. Zhu, Sci. Bull. **66**, 1288 (2021).
[12] S. S. Agaev, K. Azizi, and H. Sundu, Phys. Rev. D **95**, 114003 (2017).
[13] H. Sundu, S. S. Agaev, and K. Azizi, Phys. Rev. D **98**, 054021 (2018).
[14] S. S. Agaev, K. Azizi, and H. Sundu, Phys. Rev. D **106**, 014025 (2022).
[15] C. Chen and E. S. Norella, https://indico.cern.ch/event/1176505/.
[16] M. Bayar, A. Feijoo, and E. Oset, Phys. Rev. D **107**, 034007 (2023).
[17] T. Ji, X. K. Dong, M. Albaladejo, M. L. Du, F. K. Guo, and J. Nieves, Phys. Rev. D **106**, 094002 (2022).
[18] Q. Xin, Z. G. Wang, and X. S. Yang, AAPPS Bull. **32**, 37 (2022).
[19] J. M. Xie, M. Z. Liu, and L. S. Geng, Phys. Rev. D **107**, 016003 (2023).
[20] R. Chen and Q. Huang, arXiv:2209.05180.
[21] D. Guo, J. Z. Wang, D. Y. Chen, and X. Liu, Phys. Rev. D **106**, 094037 (2022).
[22] D. Guo, J. Li, J. Zhao, and L. He, arXiv:2211.10834.

[23] M. A. Shifman, A. I. Vainshtein, and V. I. Zakharov, Nucl. Phys. **B147**, 385 (1979).
[24] M. A. Shifman, A. I. Vainshtein, and V. I. Zakharov, Nucl. Phys. **B147**, 448 (1979).
[25] W. Chen and S. L. Zhu, Phys. Rev. D **83**, 034010 (2011).
[26] R. L. Jaffe, Phys. Rep. **409**, 1 (2005).
[27] S. S. Agaev, K. Azizi, and H. Sundu, Turk. J. Phys. **44**, 95 (2020).
[28] B. L. Ioffe, Nucl. Phys. **B188**, 317 (1981); **B191**, 591(E) (1981).
[29] B. L. Ioffe, Prog. Part. Nucl. Phys. **56**, 232 (2006).
[30] S. Narison, Nucl. Part. Phys. Proc. **270–272**, 143 (2016).
[31] R. L. Workman *et al.* (Particle Data Group), Prog. Theor. Exp. Phys. **2022**, 083C01 (2022).
[32] P. Colangelo, G. Nardulli, and N. Paver, Z. Phys. C **57**, 43 (1993).
[33] S. S. Agaev, K. Azizi, and H. Sundu, J. High Energy Phys. 06 (2022) 057.
[34] T. Feldmann, P. Kroll, and B. Stech Phys. Rev. D **58**, 114006 (1998).
[35] S. S. Agaev, V. M. Braun, N. Offen, F. A. Porkert, and A. Schäfer, Phys. Rev. D **90**, 074019 (2014).
[36] S. S. Agaev, K. Azizi, and H. Sundu, Phys. Rev. D **92**, 116010 (2015).